ACS OMEGA

http://pubs.acs.org/journal/acsodf

Article

Mechanical Properties and Biocompatibility of Ti-doped Diamond-like Carbon Films

Mengqi Zhang,[‖] Tianyi Xie,[‖] Xuzheng Qian, Ye Zhu, and Xiaomo Liu*

Cite This: *ACS Omega* 2020, 5, 22772−22777

Read Online

ACCESS | Metrics & More | Article Recommendations

ABSTRACT: A series of Ti/Ti-diamond-like carbon (Ti-DLC) films was deposited onto monocrystalline Si substrates by dual-magnetron sputtering. The mechanical properties, chemical composition, and microstructure of the films were investigated by Raman spectroscopy, X-ray photoelectron spectroscopy (XPS), scanning electron microscopy (SEM), X-ray diffraction (XRD), and nanoindentation. The biocompatibility of the Ti-DLC films was evaluated via cell viability testing. The TiC phase was formed at a Ti content of 4.43 atom %, and the surface roughness gradually increased as the Ti content increased. Ti-DLC films with 17.13 atom % Ti exhibited superior adhesion strength and surface hardness. The optical densities (ODs) of the different Ti-DLC films were similar, indicating that the films exhibit biocompatibility regardless of the Ti content. Overall, doping DLC films with Ti provides a better film for medical applications, as it improves the mechanical properties, as evidenced by the elastic modulus, hardness, adhesion strength, and surface roughness of the coating, and maintains ideal biocompatibility.

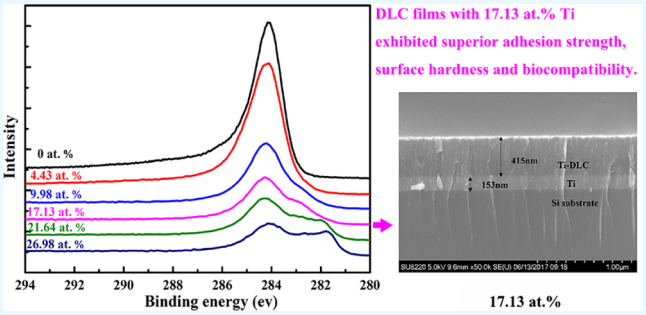

1. INTRODUCTION

A variety of medical devices such as artificial knee and hip joints, heart valves, and coronary stents are implanted in human bodies for restorative medical purposes. The material components of these devices must be compatible with the cells and fluids of the human body. However, implants without proper surface modification exhibit low wear resistance, and the debris particles generated by wear ultimately lead to tissue inflammation.[1] Metallic implants release metal ions and wear debris into the surrounding tissues, which may induce pseudotumour formation[2] and lead to osteolysis and loosening, resulting in implant failure.[3] Coating implants with protective films can reduce wear and corrosion and extend the lifetime of implants for the benefit of patients.

A diamond-like carbon (DLC) film is an attractive biomedical material owing to its high hardness, low friction coefficient, good chemical stability, and biocompatibility.[4] DLC films have been widely used to modify the surfaces of medical devices[5] such as artificial articulating joints, heart pumps and valves,[4] and biomedical implants.[6] DLC is an amorphous allotrope of carbon containing 0−40 atom % hydrogen and sp^3- and sp^2-bonded carbon atoms.[6] The sp^2 and sp^3 ratio has a strong effect on the mechanical properties of DLC films. The bioinertness of DLC has been confirmed in various studies.[7−12] For example, studies on the effects of DLC coatings on cells found no evidence of cytotoxicity,[12] and studies of the interactions of macrophages with DLC coatings have confirmed that DLC does not induce inflammatory reactions in cells. DLC has also shown excellent biocompatibility with blood monocytes;[9] this is crucial because monocytes control inflammatory reactions that can affect osteointegration of implants. However, the commercialization of DLC films has been limited by their poor adhesion[13] to substrates due to their high internal stress and chemical bonding mismatch.[14,15]

Two methods have been explored to improve the adhesive strength of DLC films: deposition of interlayers and doping.[16] To overcome the most critical issues, different coating concepts involving W, Ni, Si, and Zr have been proposed.[17−20] Ti, silicon nitride, and chromium carbide are commonly used as interlayers, as these materials potentially offer a physical barrier between corrosive environments and their substrates. However, some doping materials such as Ag may slightly reduce the coating hardness,[21] which is problematic with regard to mechanical performance. Several studies have found that NiTi alloy samples coated with TiC have better thermal dynamic stability[22] and mechanical performance.[23] Addition-

Received: April 14, 2020
Accepted: August 14, 2020
Published: August 31, 2020

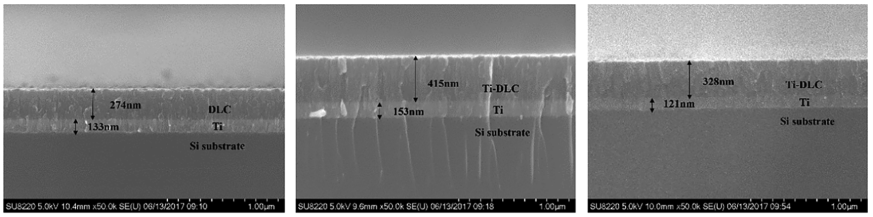

Figure 1. Cross-sectional SEM morphologies of Ti/Ti-DLC films prepared with different Ti contents.

ally, Ti coatings on stainless steel samples have been shown to reduce bacterial attachment.[24]

Ti reduces the residual stress by lowering the amount of sp^3-bonded C in the DLC matrix and improves the bonding between the coating and the substrate, preventing delamination.[25] Studies have shown that the addition of 7−13% Ti in DLC increases bone marrow cell differentiation and lowers osteoclast-like activity on coated surfaces.[26,27] Slight differences in the Ti content of Ti-DLC films may lead to variations in film properties, and a consensus is yet to be reached on the appropriate amount of Ti to obtain optimum film properties or the influence of gradient Ti doping.

To improve the properties of DLC films and determine the optimum concentration of Ti, a series of Ti/Ti-DLC films was deposited using a dual-magnetron sputtering system. The mechanical properties, chemical composition, microstructure, and biocompatibility of the films were investigated.

2. RESULTS AND DISCUSSION

2.1. Surface and Cross-sectional Morphologies. Figure 1 shows cross-sectional SEM images of the Ti/Ti-DLC films prepared with different Ti contents. The Ti interlayer and DLC top layer are clearly evident, and the two-layer structure appears to be dense. The Ti interlayer, which provides good adhesion between the DLC layer and the substrate, had a thickness of ∼135 ± 15 nm. The thicknesses of the DLC films with Ti contents of 17.13 and 26.98 atom % were 415 and 328 nm, respectively, whereas that of the pure DLC film (0 atom % Ti) was ∼274 nm. The lower thickness of the pure DLC film is possibly due to the higher growth stress.

Figure 2 shows the contrast in the three-dimensional atomic force microscopy (AFM) morphology of the Ti-DLC film as a function of the Ti doping content. All film surfaces were smooth and uniform and consisted of many small compact microparticles. Nevertheless, the surface roughness values, R_a and R_q, gradually increased with the Ti content, as summarized in Table 1. It is considered that the incorporation of Ti reduced the migration energy of C atoms, resulting in a slightly rougher film surface.

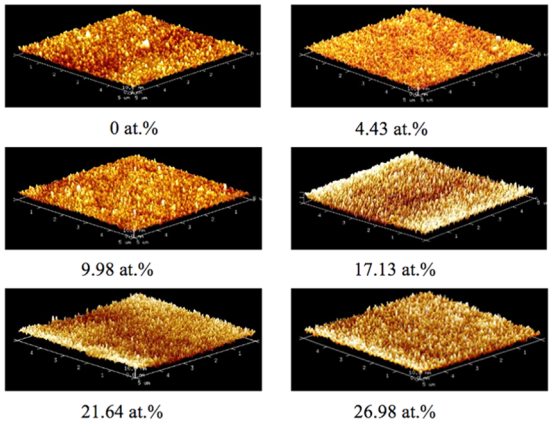

Figure 2. Typical AFM images of Ti-DLC films with different Ti contents.

Table 1. R_a and R_q Values of Ti-DLC Films Prepared with Different Ti Contents

Ti doping content (atom %)	R_a (nm)	R_q (nm)
0	1.23	1.57
4.43	1.42	1.81
9.98	1.44	1.85
17.13	2.01	2.57
21.64	2.31	2.89
26.98	2.64	3.32

2.2. Chemical Composition and Microstructure. The phase composition of the as-deposited composite films with different Ti contents was examined using X-ray diffraction (XRD); the results are shown in Figure 3. No peaks related to C or diamond were detected, suggesting that the coating matrix was amorphous. Compared with the pure DLC film, all Ti-DLC films exhibited TiC (111) peaks centered near 2θ = 36.57°; the relative intensities of these peaks gradually increased as the Ti content increased. The introduction of Ti can lead to TiC formation, and the fraction of the TiC phase is positively correlated with the Ti content.

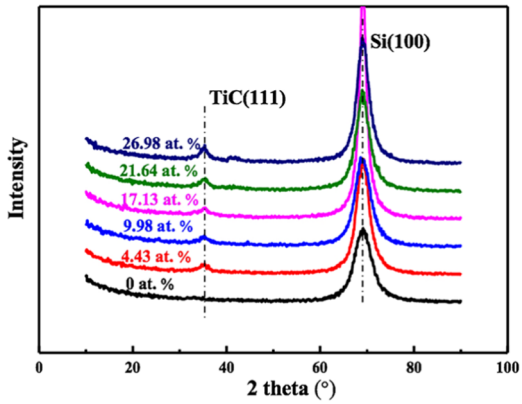

Figure 3. XRD patterns of the as-deposited Ti-DLC films with different Ti contents.

X-ray photoelectron spectroscopy (XPS) was carried out to further investigate the detailed bonding state of the Ti-DLC films. Figure 4a,b shows the Ti 2p and the C 1s XPS spectra of Ti-DLC films as a function of the Ti content, respectively. The

https://dx.doi.org/10.1021/acsomega.0c01715
ACS Omega 2020, 5, 22772−22777

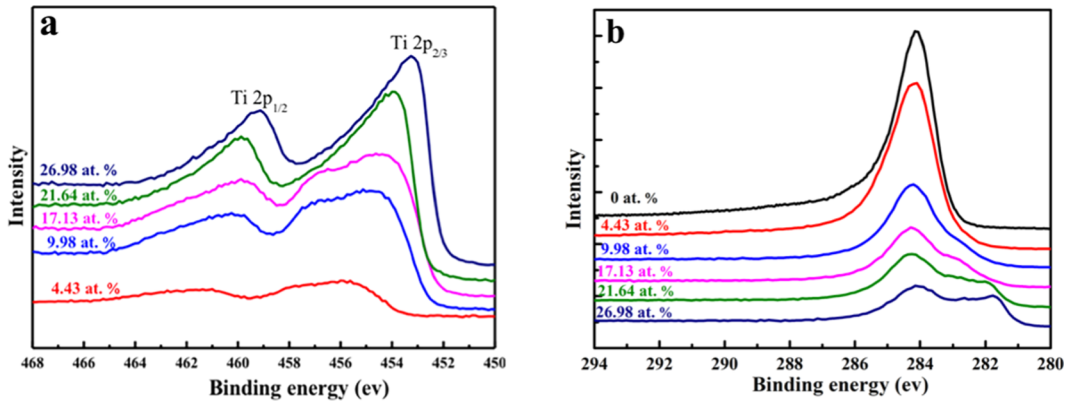

Figure 4. (a) Ti 2p and (b) C 1s X-ray photoelectron spectra of Ti-DLC films as a function of the Ti content.

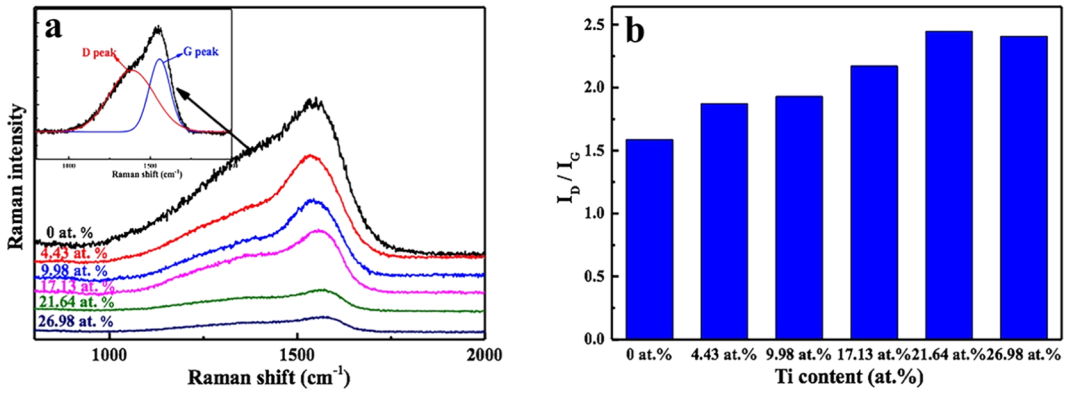

Figure 5. (a) Raman spectra and (b) ID/IG of Ti-DLC films as a function of the Ti content.

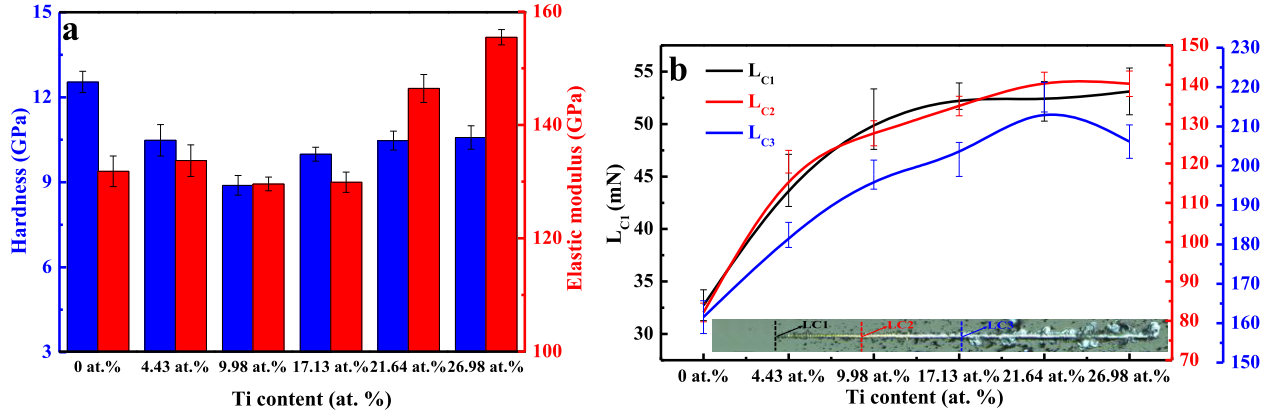

Figure 6. (a) Hardness and elastic modulus and (b) critical loads of Ti-DLC films as a function of the Ti content.

peaks near 454.2 and 460.3 eV in the Ti 2p spectrum correspond to Ti $2p^{3/2}$ and Ti $2p^{1/2}$ of pure TiC, respectively;[28,29] this indicates that Ti atoms were incorporated into the films and formed TiC. Moreover, the intensities of the peaks were relatively weak at a Ti content of 4.43 atom % and then increased with the Ti content because of the increased fraction of the TiC phase. Figure 4b shows a high-intensity C 1s peak located near 284.6 eV for the pure DLC film, whereas the peak shifted to lower binding energy with an increase in the Ti content from 0 to 26.98 atom %; this is attributed to the transformation from sp^3 to sp^2 bonding. However, the peak intensity decreased as the Ti content increased, i.e., the concentration of C decreased in the films. The samples with Ti contents of 21.64 atom % may have generated the intermediate metallic compound Ti_xC_{1-x} and a small amount of Ti oxide during the generation of TiC, resulting in a slightly higher binding energy. The XPS peak has no asymmetric peak at 281.6 eV because there is no TiC formed with Ti contents of 0 atom %. When the Ti content is 4.43 atom %, only a small amount of TiC is formed. Therefore, the XPS curve has no obvious shoulder peak at 281.6 eV. Nevertheless, the intensity of this peak was very weak in the film with a Ti content of 4.43 atom %, which is inconsistent with the XRD results. It can be inferred that below a concentration of 4.43 atom %, a small amount of Ti element exists as a simple substance in the carbon matrix because the substrate reaction temperature is not high, which plays a role in adjusting the carbon atom structure and can relieve internal stress to a certain extent, thus

https://dx.doi.org/10.1021/acsomega.0c01715
ACS Omega 2020, 5, 22772−22777

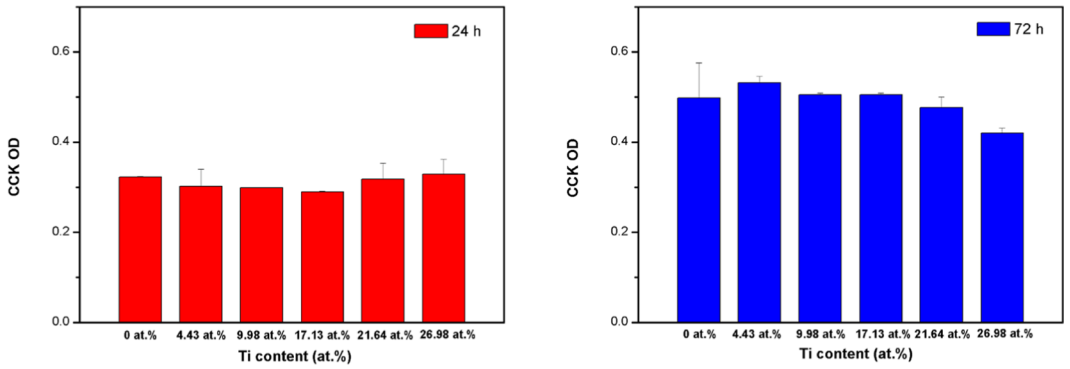

Figure 7. Cell proliferation of Ti-DLC films with different Ti contents. The data represent the mean and standard deviation (SD) values. The "*" over the bar indicates "significantly different from the control group (P, 0.05)".

the Ti dopants are mainly dissolved in the amorphous C matrix, and only a small amount of TiC is formed.

Raman spectroscopy is an effective method for studying the evolution of C atomic structures. Figure 5a shows the typical Raman spectra of the DLC films with and without Ti doping. The Raman spectra were fitted with two Gaussian peaks: the D peak at approximately 1360 cm^{-1} and the G peak at approximately 1540 cm^{-1}. It is well known that the D peak is related to the graphite structure and represents the breathing mode of sp^2 atoms in aromatic rings, whereas the G peak corresponds to the diamond structure, originating from the stretching mode of sp^3 atoms in both aromatic rings and chains. As a result, the sp^2 and sp^3 ratio can be determined from the ratio of the areas of the D and G peaks (I_D/I_G). The results are shown in Figure 5b; the I_D and I_G ratio increased as the Ti content increased from 0 to 21.64 atom % and then slightly decreased at 26.98 atom % Ti. On the basis of these findings, we can conclude that the introduction of Ti resulted in an increase in the amount of sp^2 bonding in Ti-DLC films.

2.3. Mechanical Performance. The hardness and film−substrate adhesion are two main factors that affect the mechanical properties of films; they are directly correlated with their reliability and service life. Figure 6a shows the hardness and corresponding elastic modulus as a function of the Ti content. The hardness decreased from 12.54 to 8.89 GPa as the Ti content increased from 0 to 9.98 atom %. During this stage, the Ti atoms uniformly dissolved in the amorphous C matrix and formed small amounts of nanocrystalline carbides (according to the XRD and XPS results), effectively breaking the continuity of the C network. As a result, the film hardness decreased. A further increase in the Ti content from 17.13 to 26.98 atom % resulted in an increase in the hardness from 9.98 to 10.54 GPa; this is attributed to the continuous formation of nanocrystalline carbides with the increase in the Ti content, which effectively compensated for the destruction of the C network, thus leading to an increase in the film hardness. Notably, the changes in the elastic modulus and hardness of the films were not synchronized.

In general, the critical loads L_{C1}, L_{C2}, and L_{C3} are used to characterize the adhesion strength of films, where L_{C1} is defined as the normal load at which the first crack appears in the film, L_{C2} is the load at which chipping of the film first occurs, and L_{C3} corresponds to complete delamination of the film. Figure 6b shows the relationship between the adhesion strength and the Ti content. The adhesion strength sharply increased as the Ti content increased from 0 to 17.13 atom % and then increased at a slower rate with a further increase in the Ti content. Although the hardness of the Ti-DLC film with 17.13 atom % Ti was lower than that of the pure DLC film, the adhesion strength of the former was significantly higher than that of the latter. As a result, the Ti-DLC film with a Ti content of 17.13 atom % is considered to be superior in terms of the mechanical properties.

2.4. Biocompatibility. Figure 7 shows the cytotoxicity of the Ti-DLC films. The hPDLCs proliferated favorably during the incubation period. After 24 and 72 h, the optical densities (ODs) of the control samples (DLC alone) and groups with Ti doping were not significantly different. There was also no significant difference in the ODs of the Ti-DLC films prepared with different Ti contents. Thus, doping with Ti can maintain the biocompatibility of a biomaterial over a long term and independent of the Ti content. Several dental products made of metallic materials are used in the mouth, such as restorations, braces, and implants; thus, the evaluation of hPDLCs can reflect the compatibility in the mouth well.

DLC coatings have been reported to be noncytotoxic,[10,12] and the formation of TiC has no effect on compatibility, as it has been proved that no sign of toxicity was found after the absorption of TiC.[30] The addition of Ti particles reportedly has a beneficial effect on human dental pulp stem cells and osteoblast viability.[31] Overall, doping DLC films with Ti provides a better film for medical applications, as it improves the mechanical properties, as evidenced by the elastic modulus, hardness, adhesion strength, and surface roughness of the coating, and maintains ideal biocompatibility. Thus, Ti/Ti-DLC coatings have considerable potential for applications involving bone tissue engineering, biomedical implants, soft tissue (e.g., blood vessel) repair, and so on. We hope the existing data could conclude the optimal Ti doping content considering the mechanism properties and biocompatibility. Further exploration, including high-resolution transmission electron microscopy (HRTEM) is required in the future.

3. CONCLUSIONS

We prepared Ti/Ti-DLC composite films consisting of an amorphous DLC phase with varying Ti contents. The formation of the TiC phase was initiated at a Ti content of 4.43 atom %. The surface roughness and hardness of the films increased when the Ti content exceeded 17.13 atom %. Specifically, Ti/Ti-DLC films with a Ti content of 17.13 atom % demonstrated a superior adhesion strength and surface hardness. The introduction of Ti increased the amount of sp^2-bonded carbon in Ti-DLC films. An evaluation of the cell

https://dx.doi.org/10.1021/acsomega.0c01715
ACS Omega 2020, 5, 22772−22777

viability of the Ti-DLC films indicated good biocompatibility independent of the Ti content.

4. EXPERIMENTAL SECTION

4.1. Film Preparation. A series of Ti/Ti-DLC films was deposited onto monocrystalline Si substrates by dual-magnetron sputtering using graphite and Ti targets. Using Raman spectroscopy, we confirmed that sputtering increased the ratio of sp^2 to sp^3 bonding in the films.[32] The substrate was successively cleaned with acetone, isopropanol, and deionized water. The vacuum system was first pumped to 5×10^{-4} Pa for ~45 min. Pure Ar gas was then pumped into the deposition chamber using a mass-flow controller to maintain a working pressure of 5×10^{-1} Pa. To obtain a homogeneous Ti-DLC film, the substrate stage was rotated at 6 rpm. During the deposition process, the Ti target was operated at a power of 550 W for 30 min to deposit the Ti interlayer. Subsequently, the Ti target was switched off, and the graphite target was operated at 550 W for 3 h. During C deposition, the Ti target was operated at 40, 60, 80, 100, and 120 W to vary the Ti doping content of the DLC film (Table 2).

Table 2. Deposition Parameters of Ti-DLC Films

Ti (atom %)	C target power (W)	Ti target power (W)
0	550	0
4.43	550	40
9.98	550	60
17.13	550	80
21.64	550	100
26.98	550	120

4.2. Characterization. The surface morphologies of the films were studied by scanning electron microscopy (SEM; SU8200, Hitachi, Tokyo, Japan). The chemical structure of the films, mainly including the sp^2 and sp^3 structures of the carbon-based film, and the existent state of doping element Ti existing in the carbon matrix, was characterized by Raman spectroscopy (HR-800, Horiba, Kyoto, Kyoto Prefecture, Japan; excitation wavelength: 514.5 nm). X-ray photoelectron spectroscopy (XPS; PHI Quantera II, Ulvac-Phi Inc., Kanagawa, Japan) was used to analyze the element content and existent state of the DLC film after doping. The crystalline structures of the films were examined using a Rigaku D/max-RB X-ray diffraction (XRD) system. The scanning range was 10°−90°. Continuous scanning mode was used, and the scanning speed was 2°/min. The elastic modulus and hardness of the films were measured using a nanoindentation tester (model NHT2, CSM Instruments, Needham, MA).

4.3. Cytotoxicity Evaluation. Samples were cut into rectangles (length: 14 mm; width: 7 mm) and placed in 12-well plates. The viability of human periodontal ligament cells (hPDLCs, provided by Peking University Hospital of Stomatology, Beijing, China) on the sample films was evaluated using a cell counting kit (Cell Counting Kit-8: Code: ck04, Dojindo Laboratories, Kumamoto, Japan). The hPDLCs (P7) were seeded at a concentration of 2×10^5 cells/well onto each test sample and placed in an incubator with an atmosphere of 5% CO_2 at 37 °C. After 24 and 72 h of incubation, a CCK-8 treatment was used to measure the cell viability at 37 °C for 2 h. Additionally, the optical density (OD) of the culture medium was measured for two samples from each test group, and the ODs were compared using a one-way analysis of variance (ANOVA).

AUTHOR INFORMATION

Corresponding Author

Xiaomo Liu − *Department of Orthodontics, Peking University School of Stomatology, 100081 Beijing, P. R. China*; Email: momo96@163.com

Authors

Mengqi Zhang − *Department of Orthodontics, Peking University School of Stomatology, 100081 Beijing, P. R. China*

Tianyi Xie − *Second Dental Center, Peking University School of Stomatology, 100101 Beijing, P. R. China*; orcid.org/0000-0003-1743-7439

Xuzheng Qian − *College of Mechanical and Electrical Engineering, HuangShan University, 245041 Huangshan, P. R. China*

Ye Zhu − *Department of Orthodontics, Peking University School of Stomatology, 100081 Beijing, P. R. China*

Complete contact information is available at: https://pubs.acs.org/10.1021/acsomega.0c01715

Author Contributions

‖M.Z. and T.X. contributed equally to this work.

Notes

The authors declare no competing financial interest.

ACKNOWLEDGMENTS

The project was supported by the Tribology Science Fund of State Key Laboratory of Tribology (grant no. SKLTKF19B11), and the National Natural Science Foundation of China (grant no. 81400561). We would like to acknowledge X.Q. of the group at the university for support with the investigation of the mechanical properties.

REFERENCES

(1) Dowling, D. P.; V. K, P.; Donnelly, K.; et al. Evaluation of diamond-like carbon-coated orthopaedic implants. *Diamond Relat. Mater.* **1997**, *6*, 390−393.

(2) Ebramzadeh, E.; Campbell, P. A.; Takamura, K. M.; Lu, Z.; Sangiorgio, S. N.; Kalma, J. J.; De Smet, K. A.; Amstutz, H. C. Failure modes of 433 metal-on-metal hip implants: how, why, and wear. *Orthop. Clin. North Am.* **2011**, *42*, 241−250.

(3) Grill, A. Diamond-like carbon coatings as biocompatible materials—an overview. *Diamond Relat. Mater.* **2003**, *12*, 166−170.

(4) Ueng, H. Y.; Guo, C. T. Diamond-like carbon coatings on microdrill using an ECR-CVD system. *Appl. Surf. Sci.* **2005**, *249*, 246−256.

(5) Alanazi, A.; Nojiri, C.; Kido, T.; Noguchi, T.; Ohgoe, Y.; Matsuda, T.; Hirakuri, K.; Funakubo, A.; Sakai, K.; Fukui, Y. Engineering Analysis of Diamond-Like Carbon Coated Polymeric Materials for Biomedical Applications. *Artif. Organs* **2000**, *24*, 624−627.

(6) Hauert, R.; Thorwarth, K.; Thorwarth, G. An overview on diamond-like carbon coatings in medical applications. *Surf. Coat. Technol.* **2013**, *233*, 119−130.

(7) Gutensohn, K.; Beythien, C.; Koester, R.; Bau, J.; Fenner, T.; Grewe, P.; Padmanaban, K.; Schaefer, P.; Kuehnl, P. In vitro Biocompatibility Analyses of Stents Coated with Diamond-Like Carbon by Flow Cytometry, Cell Growth Assays and Electron Microscopy. *Infus. Ther. Transfus. Med.* **2000**, *27*, 200−206.

(8) Li, D. J.; Zhang, S. J.; Niu, L. F. Influence of NH n + beam bombarding energy on structural characterization and cell attachment of CN x coating. *Appl. Surf. Sci.* **2001**, *180*, 270−279.

(9) Linder, S.; Pinkowski, W.; Aepfelbacher, M. Adhesion, cytoskeletal architecture and activation status of primary human macrophages on a diamond-like carbon coated surface. *Biomaterials* **2002**, *23*, 767−773.
(10) Thomson, L. A.; Law, F. C.; Rushton, N.; Franks, J. Biocompatibility of diamond-like carbon coating. *Biomaterials* **1991**, *12*, 37−40.
(11) Cui, F. Z.; Li, D. J. A review of investigations on biocompatibility of diamond-like carbon and carbon nitride films. *Surf. Coat. Technol.* **2000**, *131*, 481−487.
(12) Allen, M.; Law, F.; Rushton, N. The effects of diamond-like carbon coatings on macrophages, fibroblasts and osteoblast-like cells in vitro. *Clin. Mater.* **1994**, *17*, 1−10.
(13) Ozeki, K.; Masuzawa, T.; Hirakuri, K. K. The wear properties and adhesion strength of the diamond-like carbon film coated on SUS, Ti and Ni-Ti with plasma pre-treatment. *Biomed. Mater. Eng.* **2010**, *20*, 21−35.
(14) Ma, G.; Gong, S.; Lin, G.; Zhang, L.; Sun, G. A study of structure and properties of Ti-doped DLC film by reactive magnetron sputtering with ion implantation. *Appl. Surf. Sci.* **2012**, *258*, 3045−3050.
(15) Bootkul, D.; Supsermpol, B.; Saenphinit, N.; Aramwit, C.; Intarasiri, S. Nitrogen doping for adhesion improvement of DLC film deposited on Si substrate by Filtered Cathodic Vacuum Arc (FCVA) technique. *Appl. Surf. Sci.* **2014**, *310*, 284−292.
(16) Love, C. A.; Cook, R. B.; Harvey, T. J.; Dearnley, P. A.; Wood, R. J. K. Diamond like carbon coatings for potential application in biological implants—a review. *Tribol. Int.* **2013**, *63*, 141−150.
(17) Zheng, Y. F.; Liu, X. L.; Zhang, H. F. Properties of Zr−ZrC−ZrC/DLC gradient films on TiNi alloy by the PIIID technique combined with PECVD. *Surf. Coat. Technol.* **2008**, *202*, 3011−3016.
(18) Choudhury, D.; Lackner, J. M.; Major, L.; Morita, T.; Sawae, Y.; Bin Mamat, A.; Stavness, I.; Roy, C. K.; Krupka, I. Improved wear resistance of functional diamond like carbon coated Ti-6Al-4V alloys in an edge loading conditions. *J. Mech. Behav. Biomed. Mater.* **2016**, *59*, 586−595.
(19) Choudhury, D.; Lackner, J.; Fleming, R. A.; Goss, J.; Chen, J.; Zou, M. Diamond-like carbon coatings with zirconium-containing interlayers for orthopedic implants. *J. Mech. Behav. Biomed. Mater.* **2017**, *68*, 51−61.
(20) Chen, T.; Wu, X.; Ge, Z.; Ruan, J.; Lv, B.; Zhang, J. Achieving low friction and wear under various humidity conditions by co-doping nitrogen and silicon into diamond-like carbon films. *Thin Solid Films* **2017**, *638*, 375−382.
(21) Choi, H. W.; Choi, J. H.; Lee, K. R.; Ahn, J. P.; Oh, K. H. Structure and mechanical properties of Ag-incorporated DLC films prepared by a hybrid ion beam deposition system. *Thin Solid Films* **2007**, *516*, 248−251.
(22) Cheng, Y.; Zheng, Y. F. Characterization of TiN, TiC and TiCN coatings on Ti−50.6 at.% Ni alloy deposited by PIII and deposition technique. *Surf. Coat. Technol.* **2007**, *201*, 4909−4912.
(23) Zheng, Y.; Liu, D.; Liu, X.; Li, L. Ti-TiC-TiC/DLC gradient nano-composite film on a biomedical NiTi alloy. *Biomed. Mater.* **2008**, *3*, No. 044103.
(24) Zhao, Y. Y.; Zhao, B.; Su, X.; Zhang, S.; Wang, S.; Keatch, R.; Zhao, Q. Reduction of bacterial adhesion on titanium-doped diamond-like carbon coatings. *Biofouling* **2018**, *34*, 26−33.
(25) Ding, X. Z.; Tay, B. K.; Lau, S. P.; Zhang, P.; Zeng, X. T. Structural and mechanical properties of Ti-containing diamond-like carbon films deposited by filtered cathodic vacuum arc. *Thin Solid Films* **2002**, *408*, 183−187.
(26) Francz, G.; Schroeder, A.; Hauert, R.; Francz, G.; Schroeder, A.; Hauert, R.; Francz, G.; Schroeder, A.; Hauert, R. Surface analysis and bioreactions of Ti- and V-containing a-C: H. *Surf. Interface Anal.* **1999**, *28*, 3−7.
(27) Schroeder, A.; Francz, G.; Bruinink, A.; Hauert, R.; Mayer, J.; Wintermantel, E. Titanium containing amorphous hydrogenated carbon films (a-C: H/Ti): surface analysis and evaluation of cellular reactions using bone marrow cell cultures in vitro. *Biomaterials* **2000**, *21*, 449−456.
(28) Rossetti, F. F.; Ilya Reviakine, A.; Textor, M. Characterization of Titanium Oxide Films Prepared by the Template-Stripping Method. *Langmuir* **2003**, *19*, 10116−10123.
(29) Moulder, J. F.; Chastain, J.; King, R. C., Jr Handbook of x-ray photoelectron spectroscopy: a reference book of standard spectra for identification and interpretation of XPS data. *Chem. Phys. Lett.* **1992**, *220*, 7−10.
(30) Laloy, J.; Lozano, O.; Alpan, L.; Mejia, J.; Toussaint, O.; Masereel, B.; Dogné, J. M.; Lucas, S. Can TiC nanoparticles produce toxicity in oral administration to rats? *Toxicol. Rep.* **2014**, *1*, 172−187.
(31) Aguilar-Perez, F. J.; Vargas-Coronado, R.; Cervantes-Uc, J. M.; Cauich-Rodriguez, J. V.; Rosales-Ibanez, R.; Pavon-Palacio, J. J.; Torres-Hernandez, Y.; Rodriguez-Ortiz, J. A. Preparation and characterization of titanium-segmented polyurethane composites for bone tissue engineering. *J. Biomater. Appl.* **2018**, *33*, 11−22.
(32) Robertson, J. Diamond-like amorphous carbon. *Mater. Sci. Eng., R* **2002**, *37*, 129−281.

https://dx.doi.org/10.1021/acsomega.0c01715
ACS Omega 2020, 5, 22772−22777